Year-long COVID-19 infection reveals within-host evolution of SARS-CoV-2 in a patient with B cell depletion

Veronique Nussenblatt, M.D.[1*], Allison E Roder, Ph.D.[2*], Sanchita Das, M.D.[3], Emmie de Wit, Ph.D.[4], Jung-Ho Youn, Ph.D.[3], Stephanie Banakis, M.S.[2], Alexandra Mushegian, Ph.D.[2], Christopher Mederos, B.S.[2], Wei Wang, M.S.[2], Matthew Chung, Ph.D[2]., Lizzette Pérez-Pérez, M.S.[4], Tara Palmore, M.D.[5], Jennifer N. Brudno, M.D.[6], James N. Kochenderfer, M.D.[6], Elodie Ghedin, Ph.D.[2]

[1]Laboratory of Clinical Immunology and Microbiology, NIAID, NIH, Bethesda, MD 20854, USA

[2]Systems Genomics Section, Laboratory of Parasitic Diseases, DIR, NIAID, NIH, Bethesda, MD 20894, USA

[3]Department of Laboratory Medicine, NIH, Bethesda, MD 20894, USA

[4]Laboratory of Virology, DIR, NIAID, NIH, Hamilton, MT, USA

[5]Clinical Center, NIH, Bethesda, MD 20854, USA

[6]Surgery Branch, Center for Cancer Research, NCI, NIH, Bethesda, MD 20894, USA

*Contributed equally to this article

Corresponding author: elodie.ghedin@nih.gov

Key words: COVID-19, SARS-CoV-2, prolonged infection, immunocompromised, viral evolution

Summary: We report an immunocompromised patient with persistent symptomatic SARS-CoV-2 infection for 335 days. During this time, the virus accumulated a unique in-frame deletion in the spike, and a complete deletion of ORF7b and ORF8 which is the first report of its kind in an immunocompromised patient.

ABSTRACT

Background: B-cell depleting therapies may lead to protracted disease and prolonged viral shedding in individuals infected with SARS-CoV-2. Viral persistence in the setting of immunosuppression raises concern for viral evolution.

Methods: Amplification of sub-genomic transcripts for the E gene (sgE) was done on nasopharyngeal samples over the course of 355 days in a patient infected with SARS-CoV-2 who had previously undergone CAR T cell therapy and had persistently positive SARS-CoV-2 nasopharyngeal swabs. Whole genome sequencing was performed on samples from the patient's original presentation and 10 months later.

Results: Over the course of almost a year, the virus accumulated a unique in-frame deletion in the amino-terminal domain of the spike protein, and complete deletion of ORF7b and ORF8, the first report of its kind in an immunocompromised patient. Also, minority variants that were identified in the early samples—reflecting the heterogeneity of the initial infection—were found to be fixed late in the infection. Remdesivir and high-titer convalescent plasma treatment were given, and the infection was eventually cleared after 335 days of infection.

Conclusions: The unique viral mutations found in this study highlight the importance of analyzing viral evolution in protracted SARS-CoV-2 infection, especially in immunosuppressed hosts, and the implication of these mutations in the emergence of viral variants.

BACKGROUND

Cell-mediated and humoral immunity are necessary to clear SARS-CoV-2 infection [1, 2]. Individuals receiving B-cell depleting therapies can have protracted disease and prolonged viral shedding [3-6]. Persistent shedding of viral RNA for weeks to months after onset of symptoms has been reported, however viable virus is not detected after 9 days post illness onset in most patients [7]. In contrast, viral replication has been detected in immunocompromised patients for several months after initial infection [5, 8, 9]. Persistent viral replication in these patients is likely the result of profound lymphocyte defects due to B- and T-cell depleting therapies or underlying hematologic disease. Viral persistence in the setting of immunosuppression has raised concern for viral evolution [9] and the emergence of variants, especially during treatment with convalescent plasma [6].

Recent studies have demonstrated that SARS-CoV-2 in immunocompromised hosts is prone to significant deletion mutations in the spike protein, especially in the S1 region [5, 8, 9]. Deletions across the genome can reflect virus-host interactions and are found in both immunocompetent and immunosuppressed hosts. For example, accessory proteins ORF7ab and ORF8, which are associated with early stimulation of IFN-γ production [10], were found to be deleted in a substantial number of immune competent individuals.

Here, we report a patient with persistent symptomatic viral infection over a period of at least 335 days. Viral genome sequencing revealed the emergence of a unique in-frame deletion in the amino-terminal domain (NTD) of the spike protein, and a complete deletion of the ORF7b and ORF8 coding regions; such a large deletion of the ORF7b-ORF8 region of the genome is the first report of its kind in an immunocompromised patient. Remdesivir and high-titer convalescent plasma treatment were administered after the appearance of deletion mutations in the virus genome, with subsequent clearance of the infection.

METHODS

Approvals

Written consent was obtained for human research subjects, as approved by the NIH Institutional Review Board (protocol # NCT02659943). The patient consented to have the results of this research published.

SARS-CoV-2 RNA and sgRNA qPCR

Detection of the N gene or ORF1a/b was performed as part of diagnostic testing on all specimens collected. Amplification of sub-genomic transcripts for the E gene (sgE) was done prospectively on samples after day 275 and retrospectively on 19 samples prior to day 275, following methods described previously [8].

SARS-CoV-2 amplification, library preparation and sequencing

Amplification of viral genomes was done with custom tiling primers using a modified version of the ARTIC consortium protocol for nCoV-2019 sequencing (https://artic.network/ncov-2019) and the methods described in *Roder et al 2021* [15]. All libraries were prepared using the Nextera XT library preparation kit (Nextera), scaled down to 0.25x of the manufacturer's instructions and libraries were sequenced on the Illumina NextSeq500 using the 2x300 bp paired end protocol.

Genome assembly, generation of consensus sequences and identification of variants

Following sequencing, Illumina sequencing adapters and primer sequences were trimmed with Trimmomatic v0.36 [16]. The trimmed reads were aligned to the Wuhan-Hu-1 SARS-CoV-2 reference genome (NC_045512.2) using BWA mem v0.7.17 with the -K parameter set to 100000000 for reproducibility and -Y to use soft clipping for supplementary alignments [17]. The two primer pool libraries for each biological sample were merged into one alignment file using

73 Picard Tools MergeSamFiles v2.17.11. Duplicates were marked using GATK
74 MarkDuplicatesSpark v4.1.3.0 (https://gatk.broadinstitute.org/hc/en-us/articles/360037224932-
75 MarkDuplicatesSpark). The pipeline used to analyze the data is available at
76 https://github.com/gencorefacility/covid19. Consensus sequences, consensus mutations and
77 minority variants were called using an in-house variant calling pipeline, *timo*, which is available at
78 https://github.com/GhedinLab/timo. Minority variants were called if present at or above an allele
79 frequency of 0.02 and a coverage of 200X.
80
81 Generation of phylogenetic trees and lineage identification
82 Phylogenetic trees were generated using the Nextstrain software package and default parameters
83 [18]. A total of 266 sequences from Maryland collected between April 2020 and March 2021 were
84 downloaded from GISAID and included as background and are available in supplementary table
85 1 [19]. Lineages were called using Nextclade and Pangolin software packages [18, 20, 21].
86
87 **RESULTS**
88 *Case presentation* - A woman in her 40's with type II diabetes mellitus and diffuse large B-cell
89 lymphoma (DLBCL), who had been in complete remission for three years, presented with fever,
90 headache, nasal congestion, and productive cough. She reported that her symptoms developed
91 eleven days prior to presentation. The patient's history is relevant for treatment with multiple lines
92 of therapy and anti-CD19 chimeric antigen receptor-modified T-cell (CAR-T) therapy [11] three
93 years prior, resulting in ongoing B-cell aplasia, hypogammaglobulinemia, CD4 lymphopenia, and
94 recurrent upper respiratory infections. A previous attempt at intravenous immunoglobulin therapy
95 (IVIG) replacement was complicated by infusion reactions, after which the patient intermittently
96 declined prophylactic IVIG.
97 A chest computerized tomography (CT) exam performed on admission showed scattered,
98 bilateral, ground-glass radiodensities and consolidations and she required 2L of supplemental

99 oxygen via nasal cannula (NC). Laboratory evaluation revealed a white blood cell count of 4.67 x
100 10^9 cells/L (3.98 x 10^9 cells/L-10.04 x 10^9 cells/L), absolute lymphocyte count of 0.81 x 10^9 cells/L
101 (1.18 x 10^9 cells/L-3.74 x 10^9 cells/L), absolute neutrophil count of 3.41 x 10^9 cells/L (1.56 x 10^9
102 cells/L-6.13 x 10^9 cells/L), IgG of 144 mg/dL (700-1600mg/dL), IgM 12 mg/dL (40-230 g/dL), IgA
103 31mg/dL (70-400mg/dL), CD4 count of 202/mcl. Nasopharyngeal (NP) swabs were negative for
104 SARS-CoV-2 PCR on three occasions prior to presentation. Her symptoms worsened and she
105 required 5L of supplemental oxygen via NC. Due to her worsening clinical status, bronchoalveolar
106 lavage (BAL) was performed on Day 1 (May 2020). Broad microbiological testing of the BAL fluid
107 was negative, except a positive PCR test for SARS-CoV-2. The patient's supplemental oxygen
108 requirement increased to 60% FiO_2 and flow of 40 liters/minute (LPM) via high flow nasal cannula
109 and a vasopressor was initiated, in addition to broad spectrum antibiotics. On Day 2, she received
110 convalescent plasma and 40g of 10% immune globulin IV for her underlying
111 hypogammaglobulinemia. She did not receive remdesivir as it was not available at the time of
112 initial disease presentation. Corticosteroids were not administered as robust clinical trial data
113 regarding their use in the acute setting of COVID-19 was not yet available.

114 The patient was discharged a month later with temperatures of 99-100°F, episodes of
115 worsening cough and 3L NC supplemental oxygen. Testing for SARS-CoV-2 by PCR on NP
116 swabs was performed monthly for 3 months and every 3 months, thereafter. These were positive
117 intermittently with Ct values ranging between 37 and 38 (**Fig. 1**). Due to the patient's overall mild
118 to absent symptoms, positive SARS-CoV-2 tests during this period were thought to probably
119 reflect shedding of non-viable virus particles; however, repeat chest CTs over the same period
120 showed bilateral increasing multifocal ground-glass opacities with crazy paving pattern and mixed
121 changes. At this time, organizing pneumonia and superimposed bacterial or fungal infection were
122 considered. The patient preferred conservative management and declined bronchoscopy to rule
123 out a superimposed infection. Induced sputum was negative for bacterial, fungal, or mycobacterial
124 pathogens.

125

126 On Day 242, prednisone 50mg daily was initiated for the treatment for COVID-19-related
127 cryptogenic organizing pneumonia and resulted in moderate symptom and slight radiographic
128 improvement. SARS-CoV-2 PCR from a NP sample on day 284 was positive with a Ct value of
129 27.5, a marked decrease from the Ct value of 38 on day 197, indicating a substantial increase in
130 viral load. This viral load increase in the setting of steroids and only modest decrease in symptoms
131 was concerning for SARS-CoV-2 relapse versus new infection. A Ct value of 32.7 from sub-
132 genomic RNA (sgRNA) real-time PCR performed at this time indicated recent virus replication
133 [12-14] (**Fig. 1**). SARS-CoV-2 antibody testing was also performed but was negative. Shortly after,
134 the patient reported worsening of respiratory symptoms with new oxygen requirement of 6L NC
135 at rest. C-reactive protein (CRP) had been 37-80mg/L (<3.0 mg/L) and rose to 144mg/L after
136 prednisone initiation. She was admitted to the hospital on Day 313 and treated with high-titer
137 convalescent plasma and a 10-day course of remdesivir. She was finally discharged on Day 324
138 (March 2021) on 3-4L/min of oxygen at rest and 6L/min with exertion. Prednisone was tapered to
139 physiologic doses of hydrocortisone. Three months later, CRP had normalized, CT chest showed
140 significant decrease in ground glass opacities and the patient no longer needed supplemental
141 oxygen at rest.

142

143 *Genomic analyses* - Since diagnostic testing for SARS-CoV-2 indicated high viral load in this
144 patient 10 months after initial diagnosis, we did whole genome sequencing on five samples from
145 the patient's original presentation and two samples from her second presentation to determine if
146 re-infection had occurred. Assembled consensus sequences of virus genomes were assigned
147 lineage and all samples from this patient mapped to the Pango lineage B.1.332 (Nextclade lineage
148 20C). Global surveillance of SARS-CoV-2 genomes reveals that B.1.332 was circulating at the
149 time of her initial presentation but was no longer prevalent by the time of her second presentation
150 [20, 21]. Consensus sequences were mapped onto a phylogenetic tree containing 266

151 background samples from Maryland from the time of the first to the second presentation using the
152 publicly available Nextstrain software package [18]. All samples from this patient clustered on the
153 same branch of the tree, with no intermixed background samples, indicative of a prolonged
154 infection over 335 days, rather than a re-infection event (**Fig. 2**).

155 The original sample, taken on Day 1, contained 11 consensus changes from the
156 Wuhan/Hu-1 strain (NC_045512.2). To visualize evolution of the virus over time within the patient,
157 we compared the consensus nucleotides in the later 6 samples to that of the first sample (Day 1).
158 Other samples collected the first month of infection had between 1-5 consensus changes
159 compared to the initial sample, whereas the later samples (Days 313-331) had 28 (Day 313) and
160 26 (Day 314) consensus changes at the nucleotide level from the initial sample. Of those, 19 and
161 17, respectively, were non-synonymous, with four substitutions in the spike protein (**Fig. 3A**).
162 More interestingly, the later samples contained 2 deletions: a gap at nt 22290 to 22298 that led
163 to a unique del244-246 and, consequently, a A243G substitution (**Fig. 3B**); and a 497nt deletion
164 spanning the entire length of the ORF7b coding region and all but two amino acids of the ORF8
165 (**Fig. 3C**). Of note, several of the amino acid changes identified in the later samples (days 313
166 and 314) were present as minority variants in the initial samples, suggesting a heterogeneous
167 infection early on (**Fig. 3D**, smaller circles) with eventual fixation, as observed for ORF1a:
168 A3070V, ORF7a: S37F, and N: P365L. Conversely, a consensus change present in the early
169 samples also existed as minority variant in the last sample on Day 335 (**Fig. 3D**, smaller circles).
170 The observed number of consensus changes in the later samples from the initial sample indicates
171 that the virus evolved within this patient at approximately the same evolutionary rate that has been
172 reported for SARS-CoV-1 [22], and for SARS-CoV-2 in the global population [23], estimated to be
173 around 2 fixed mutations per month.

174

175 **CONCLUSIONS**

The sequencing data clearly indicate that the patient exhibited a prolonged infection over a 335-day period, the longest reported infection with SARS-CoV-2 to date. The existence of ongoing infection is further illustrated by significant clinical improvement and normalization of CRP after viral clearance, and the fact that the virus has largely followed an evolutionary trajectory that would be expected based on the mutation rate of the polymerase. While the patient displayed COVID19-like symptoms over the entirety of the infection, lower respiratory samples that may have demonstrated ongoing viral replication in between the patient's two admissions were not available. Consequently, we cannot definitively attribute all the lung findings to infection.

Over the course of the 335-day infection, the virus accumulated mutations at approximately the same rate as expected based on the error rate of the polymerase. This was not surprising given that in both immunocompetent and immunocompromised hosts the error rate of the polymerase is likely to remain constant, though which mutations are selected for may differ due to the lack of immune pressure on the virus. Two important deletions were identified in the later samples, one in the spike protein, and one in the ORF7b and ORF8 regions. The specific NTD deletion in the spike protein that targeted residues at positions 244-246—a range that appears unique, especially for an early lineage—would impact the supersite and could induce resistance against NTD-directed antibodies [24]. This type of deletion has also been observed in variant B.1.351 (Lambda), which contains NTD deletion 242-244 and a R246I mutation [24]. It is unclear why a deletion in that region of the NTD would appear in an immunocompromised patient, but it supports previous observations where chronic SARS-CoV-2 infection in severely immunocompromised hosts receiving convalescent plasma can lead to variant emergence and reduced sensitivity to neutralizing antibodies [6]. Additionally, our patient received convalescent plasma during her first admission

The 497nt deletion in the ORF7b and ORF8 genes is the longest deletion reported in this region of the genome, and the first to be observed in an immunocompromised patient. Other reported ORF7b/ORF8 deletions in this region span from 62nt to 382nt, with the first instance

202 identified in Singapore in January of 2020 [25, 26]. *In vitro* analyses of similar deletions indicated
203 that deletion mutants had higher titers but similar levels of cytopathic effect and showed that the
204 virus was still transmissible. However, the deletion mutant may be less effective at establishing
205 infection in a new host due to loss of immune evasion features of ORF8 [26]. ORF8 has been
206 established as a key antagonist of innate immunity and has been shown to elicit a robust and
207 highly specific immune response during infection, suggesting that the deletion in competent hosts
208 may be due to immune driven selection [27]. Thus, it was surprising to see emergence of this
209 large deletion in our immunocompromised patient. It is possible that the immunocompromised
210 nature of this patient removes a need for ORF8 during infection. This hypothesis is supported by
211 data that show ORF8 is particularly tolerant to mutation, acquiring many missense and nonsense
212 mutations. ORF8 was also shown to be dispensable in cell culture [28]. A retrospective cohort
213 study performed on patients in Singapore found that some patients carried a mix of wild-type and
214 a 382nt deletion mutant in the ORF7-ORF8 region, while others only had the deletion mutant.
215 Over time, the deletion mutant outcompeted the non-deletion virus [29]. In our study, we also
216 found evidence of a mixed infection with deletion and non-deletion mutants in the Day 313 sample,
217 but infection with only the deletion mutant on Day 314, indicating that the same competition may
218 have occurred in this patient with rapid clearance of the wild-type virus (**Fig. 3C**).
219 This case demonstrates that severely immunocompromised patients may experience
220 protracted SARS-CoV-2 infection with mild symptoms and persistent virus replication. Our case
221 also highlights the limitations of SARS-CoV-2 testing, especially for lower respiratory tract
222 disease, as access to a BAL specimen may have alerted us earlier to ongoing infection. Further
223 research is necessary to understand the evolution of SARS-CoV-2 in immunocompromised hosts,
224 especially in relation to implications for viral transmission and variant emergence.
225
226
227 **ACKNOWLEDGEMENTS**

This work was funded in part by the Division of Intramural Research (DIR) at the National Institute of Allergy and Infectious Diseases of the NIH. We thank the Department of Laboratory Medicine staff for processing clinical specimens and providing technical assistance. This work utilized the computational resources of the NIH HPC Biowulf cluster (http://hpc.nih.gov).

DATA AVAILABILITY

Data is available in NCBI GenBank under the following accession numbers: MZ385697-MZ385702 and MW990333.

CONFLICTS OF INTEREST

Dr. Jennifer Brudno is on the scientific advisory board for Kyverna Therapeutics, Inc. This is an unpaid position.

Dr. James Kochenderfer: Research funding and patent royalties from Kite Pharma, a Gilead Company

257 REFERENCES

258 1. Zohar, T. and G. Alter, *Dissecting antibody-mediated protection against SARS-CoV-2.* Nat
259 Rev Immunol, 2020. **20**(7): p. 392-394.
260 2. Sekine, T., et al., *Robust T Cell Immunity in Convalescent Individuals with Asymptomatic*
261 *or Mild COVID-19.* Cell, 2020. **183**(1): p. 158-168 e14.
262 3. Karatas, A., et al., *Prolonged viral shedding in a lymphoma patient with COVID-19 infection*
263 *receiving convalescent plasma.* Transfus Apher Sci, 2020. **59**(5): p. 102871.
264 4. Kenig, A., et al., *Treatment of B-cell depleted COVID-19 patients with convalescent plasma*
265 *and plasma-based products.* Clin Immunol, 2021. **227**: p. 108723.
266 5. Hensley, M.K., et al., *Intractable COVID-19 and Prolonged SARS-CoV-2 Replication in a*
267 *CAR-T-cell Therapy Recipient: A Case Study.* Clin Infect Dis, 2021.
268 6. Kemp, S.A., et al., *SARS-CoV-2 evolution during treatment of chronic infection.* Nature,
269 2021. **592**(7853): p. 277-282.
270 7. Cevik, M., et al., *SARS-CoV-2, SARS-CoV, and MERS-CoV viral load dynamics, duration of*
271 *viral shedding, and infectiousness: a systematic review and meta-analysis.* Lancet
272 Microbe, 2021. **2**(1): p. e13-e22.
273 8. Avanzato, V.A., et al., *Case Study: Prolonged Infectious SARS-CoV-2 Shedding from an*
274 *Asymptomatic Immunocompromised Individual with Cancer.* Cell, 2020. **183**(7): p. 1901-
275 1912 e9.
276 9. Choi, B., et al., *Persistence and Evolution of SARS-CoV-2 in an Immunocompromised Host.*
277 N Engl J Med, 2020. **383**(23): p. 2291-2293.
278 10. Tan, A.T., et al., *Early induction of functional SARS-CoV-2-specific T cells associates with*
279 *rapid viral clearance and mild disease in COVID-19 patients.* Cell Rep, 2021. **34**(6): p.
280 108728.
281 11. Brudno, J.N., et al., *Safety and feasibility of anti-CD19 CAR T cells with fully human binding*
282 *domains in patients with B-cell lymphoma.* Nat Med, 2020. **26**(2): p. 270-280.
283 12. Wolfel, R., et al., *Virological assessment of hospitalized patients with COVID-2019.* Nature,
284 2020. **581**(7809): p. 465-469.
285 13. Kim, D., et al., *The Architecture of SARS-CoV-2 Transcriptome.* Cell, 2020. **181**(4): p. 914-
286 921 e10.
287 14. Speranza, E., et al., *Single-cell RNA sequencing reveals SARS-CoV-2 infection dynamics in*
288 *lungs of African green monkeys.* Sci Transl Med, 2021. **13**(578).
289 15. Roder, A.E., et al., *Diversity and selection of SARS-CoV-2 minority variants in the early New*
290 *York City outbreak.* bioRxiv, 2021.
291 16. Bolger, A.M., M. Lohse, and B. Usadel, *Trimmomatic: a flexible trimmer for Illumina*
292 *sequence data.* Bioinformatics, 2014. **30**(15): p. 2114-20.
293 17. Li, H. and R. Durbin, *Fast and accurate short read alignment with Burrows-Wheeler*
294 *transform.* Bioinformatics, 2009. **25**(14): p. 1754-60.
295 18. Hadfield, J., et al., *Nextstrain: real-time tracking of pathogen evolution.* Bioinformatics,
296 2018. **34**(23): p. 4121-4123.
297 19. Elbe, S. and G. Buckland-Merrett, *Data, disease and diplomacy: GISAID's innovative*
298 *contribution to global health.* Glob Chall, 2017. **1**(1): p. 33-46.

20. Rambaut, A., et al., *A dynamic nomenclature proposal for SARS-CoV-2 lineages to assist genomic epidemiology.* Nat Microbiol, 2020. **5**(11): p. 1403-1407.
21. Rambaut, A., et al., *Addendum: A dynamic nomenclature proposal for SARS-CoV-2 lineages to assist genomic epidemiology.* Nat Microbiol, 2021. **6**(3): p. 415.
22. Zhao, Z., et al., *Moderate mutation rate in the SARS coronavirus genome and its implications.* BMC Evol Biol, 2004. **4**: p. 21.
23. Worobey, M., et al., *The emergence of SARS-CoV-2 in Europe and North America.* Science, 2020. **370**(6516): p. 564-570.
24. Cerutti, G., et al., *Potent SARS-CoV-2 neutralizing antibodies directed against spike N-terminal domain target a single supersite.* Cell Host Microbe, 2021. **29**(5): p. 819-833 e7.
25. Gong, Y.N., et al., *SARS-CoV-2 genomic surveillance in Taiwan revealed novel ORF8-deletion mutant and clade possibly associated with infections in Middle East.* Emerg Microbes Infect, 2020. **9**(1): p. 1457-1466.
26. Su, Y.C.F., et al., *Discovery and Genomic Characterization of a 382-Nucleotide Deletion in ORF7b and ORF8 during the Early Evolution of SARS-CoV-2.* mBio, 2020. **11**(4).
27. Hachim, A., et al., *ORF8 and ORF3b antibodies are accurate serological markers of early and late SARS-CoV-2 infection.* Nat Immunol, 2020. **21**(10): p. 1293-1301.
28. Pereira, F., *Evolutionary dynamics of the SARS-CoV-2 ORF8 accessory gene.* Infect Genet Evol, 2020. **85**: p. 104525.
29. Young, B.E., et al., *Effects of a major deletion in the SARS-CoV-2 genome on the severity of infection and the inflammatory response: an observational cohort study.* Lancet, 2020. **396**(10251): p. 603-611.

334 FIGURE LEGENDS:
335
336 **Figure 1. Timeline of diagnostic tests for SARS-CoV-2 and treatment**. Nasopharyngeal or
337 oropharyngeal (upper respiratory) specimens were collected for detection of SARS-CoV-2 RNA,
338 except when indicated by the following: # indicates BAL sample, * indicates days when sputum
339 specimens were collected and † indicates days when saliva was collected. Specimens with Ct
340 values over 40 were considered negative for SARS-CoV-2 RNA. PCR for sub-genomic RNA was
341 performed only on specimens that tested positive for genomic RNA. Samples that were used for
342 next-generation sequencing are indicated with an orange circle. Treatments administered are
343 indicated with a black arrow and labeled.
344
345 **Figure 2. Phylogeny of sequenced samples.** Maximum likelihood timed strain tree
346 reconstructed from 266 local sequences from GISAID (**Table S1**). Samples sequenced from the
347 patient in this case study are colored in purple and labeled with the day of infection from first
348 diagnosis.
349
350 **Figure 3. Mutations and deletions in sequenced samples over time. (A)** Tile plot showing
351 consensus changes across the genome as compared to the initial infectious sample (collec
352 date: 2020-05-01, day 1), color-coded by residue. **(B)** Schematic showing 9 nt deletion in Spike
353 region (ntpos: 22290-22299, spike aa positions shown). **(C)** Coverage plot, tile plot and schematic
354 showing the 497nt deletion in the ORF7b and ORF8 coding regions. Coverage plot represents
355 log10 raw coverage. Dotted line is at 5X coverage. Tile plot represents amino acid changes in
356 this region, as compared to initial infectious sample (day 1), colored by residue as above in 3A.
357 Deletions identified in previous studies are shown as schematics and labeled by their country of
358 origin. **(D)** Circle plot showing major (larger, outer circle) and minor (smaller, inner circle) at
359 locations where a minority variant in one sample exists as a major amino acid in another sample,
360 colored by residue as in 3A. ORFs and aa positions within the encoded protein are listed.

Figure 1

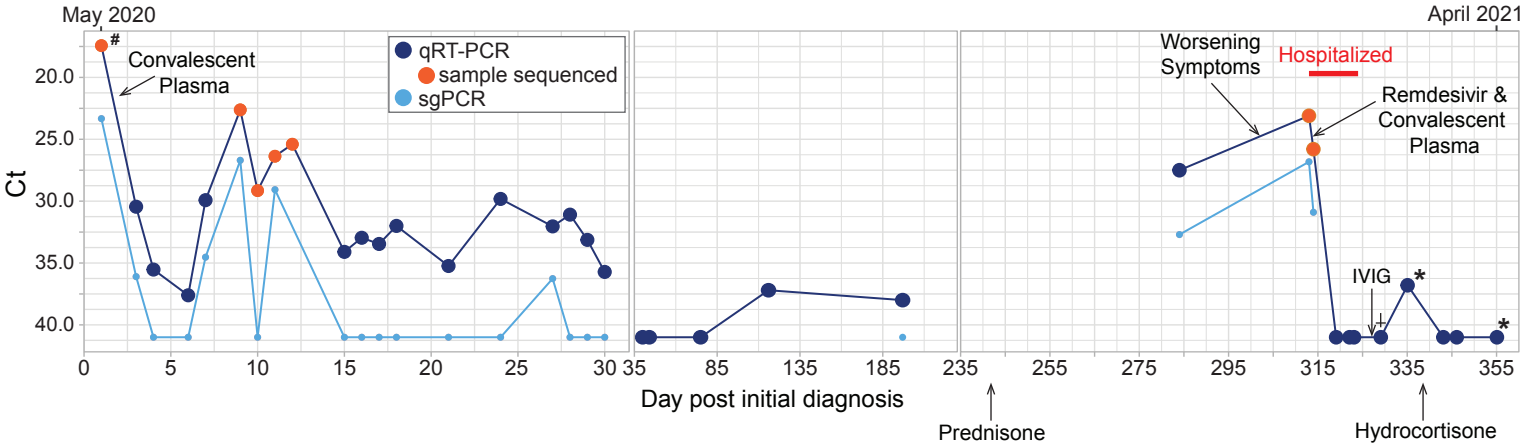
May 2020
April 2021
Convalescent Plasma
qRT-PCR
sample sequenced
sgPCR
Worsening Symptoms
Hospitalized
Remdesivir & Convalescent Plasma
IVIG
Ct
20.0
25.0
30.0
35.0
40.0
0
5
10
15
20
25
30
35
85
135
185
235
255
275
295
315
335
355
Day post initial diagnosis
Prednisone
Hydrocortisone

Figure 2

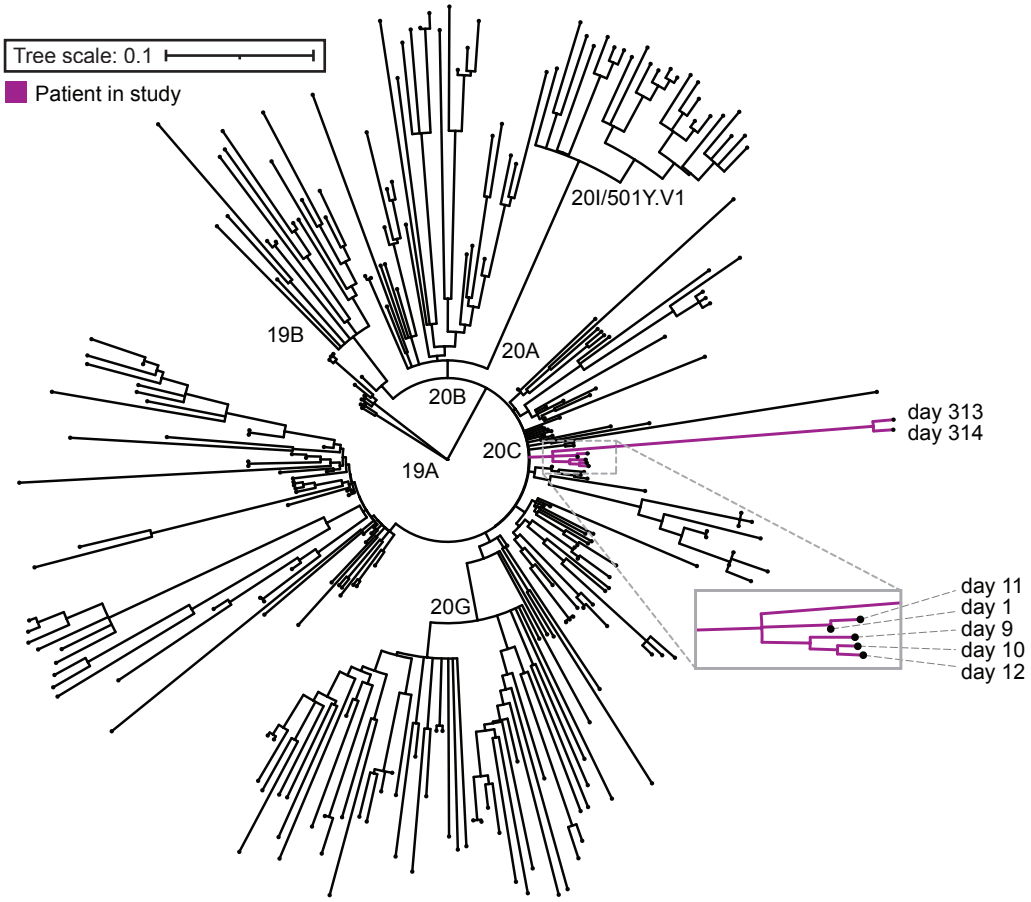
Tree scale: 0.1
Patient in study
20I/501Y.V1
19B
20A
20B
20C
19A
20G
day 313
day 314
day 11
day 1
day 9
day 10
day 12

Figure 3

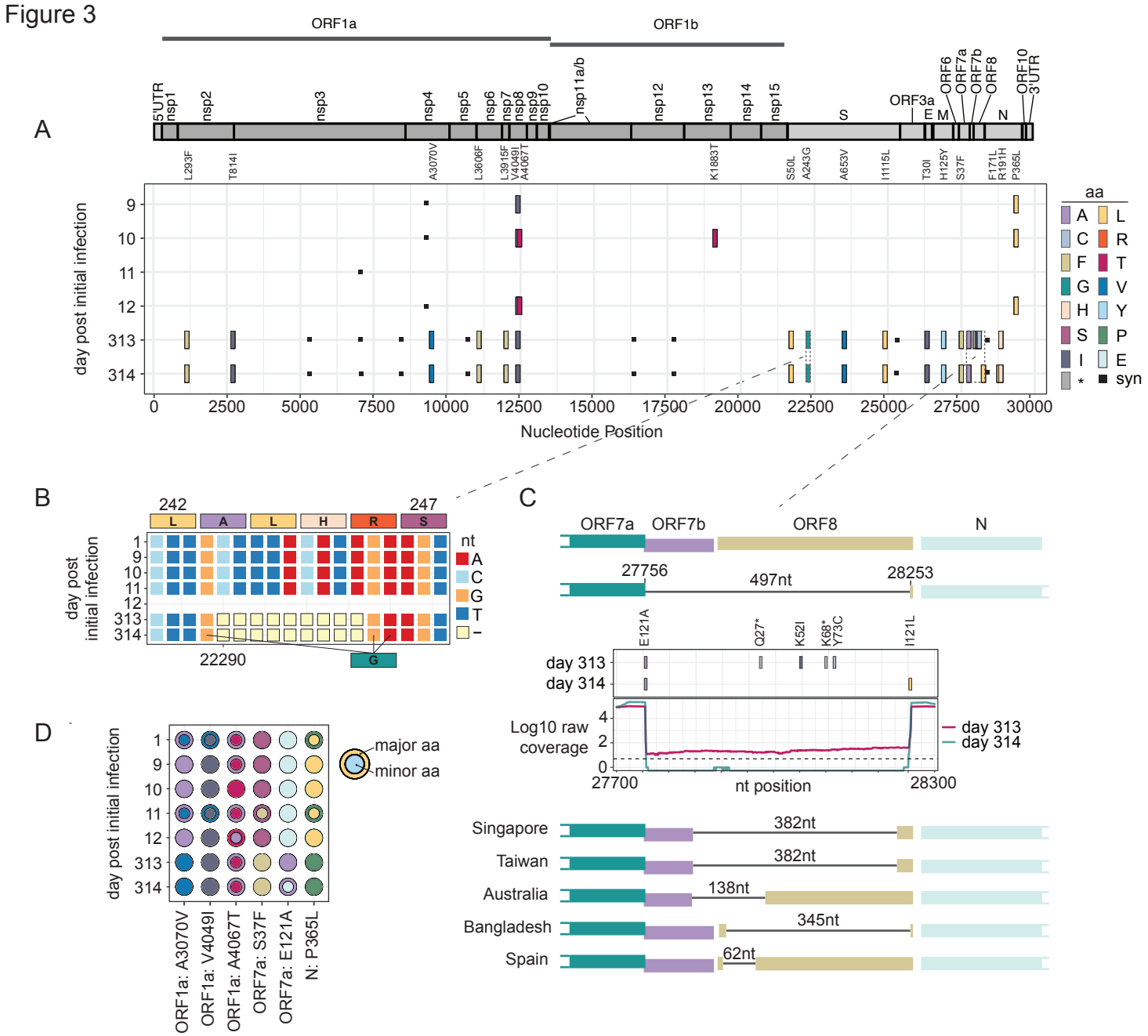
A
ORF1a
ORF1b
5'UTR
nsp1
nsp2
nsp3
nsp4
nsp5
nsp6
nsp7
nsp8
nsp9
nsp10
nsp11a/b
nsp12
nsp13
nsp14
nsp15
S
ORF3a
E
M
ORF6
ORF7a
ORF7b
ORF8
N
ORF10
3'UTR
L293F
T814I
A3070V
L3606F
L3915F
V4049I
A4067T
K1883T
S50L
A243G
A653V
I1115L
T30I
H125Y
S37F
F171L
R191H
P365L
day post initial infection
9
10
11
12
313
314
0
2500
5000
7500
10000
12500
15000
17500
20000
22500
25000
27500
30000
Nucleotide Position
aa
A
C
F
G
H
S
I
*
L
R
T
V
Y
P
E
syn
B
242
247
L
A
L
H
R
S
day post initial infection
1
9
10
11
12
313
314
22290
G
nt
A
C
G
T
–
C
ORF7a
ORF7b
ORF8
N
27756
497nt
28253
E121A
Q27*
K52I
K68*
Y73C
I121L
day 313
day 314
Log10 raw coverage
4
2
0
27700
nt position
28300
day 313
day 314
Singapore
382nt
Taiwan
382nt
Australia
138nt
Bangladesh
345nt
Spain
62nt
D
day post initial infection
1
9
10
11
12
313
314
major aa
minor aa
ORF1a: A3070V
ORF1a: V4049I
ORF1a: A4067T
ORF7a: S37F
ORF7a: E121A
N: P365L